

ANALYTICAL SOLUTION OF REACTION-DIFFUSION EQUATIONS FOR CALCIUM WAVE PROPAGATION IN A STARBURST AMACRINE CELL

R. R. POZNANSKI

*Neural Networks Research Group
Faculty of Computer Science and Information Technology
University of Malaya, 50603 Kuala Lumpur, Malaysia
roman.poznanski@um.edu.my*

Received 10 August 2010

Accepted 20 August 2010

A reaction-diffusion model is presented to encapsulate calcium-induced calcium release (CICR) as a potential mechanism for somatofugal bias of dendritic calcium movement in starburst amacrine cells. Calcium dynamics involves a simple calcium extrusion (pump) and a buffering mechanism of calcium binding proteins homogeneously distributed over the plasma membrane of the endoplasmic reticulum within starburst amacrine cells. The system of reaction-diffusion equations in the excess buffer (or low calcium concentration) approximation are reformulated as a nonlinear Volterra integral equation which is solved analytically via a regular perturbation series expansion in response to calcium feedback from a continuously and uniformly distributed calcium sources. Calculation of luminal calcium diffusion in the absence of buffering enables a wave to travel at distances of $120\ \mu\text{m}$ from the soma to distal tips of a starburst amacrine cell dendrite in 100 msec, yet in the presence of discretely distributed calcium-binding proteins it is unknown whether the propagating calcium wave-front in the somatofugal direction is further impeded by endogenous buffers. If so, this would indicate CICR to be an unlikely mechanism of retinal direction selectivity in starburst amacrine cells.

Keywords: Buffer; calcium; starburst amacrine cells; directional selectivity; retina; reaction-diffusion equations; CICR-based Ca^{2+} waves; fire-diffuse-fire model; endoplasmic reticulum; lumen; diffusion speed.

1. Introduction

Calcium (Ca^{2+}) as intracellular messenger in starburst amacrine cells (SACs) can be observed as propagating waves, which are critically involved in direction of image motion in the rabbit retina (see [19, 20] for an overview). Euler and colleagues showed that a single SAC displayed directionally selective signals by recording optically the intracellular Ca^{2+} concentrations in the intact retina [4]. These signals tended to be greater for somatofugal than somatopetal stimuli. What is the mechanism by which the SACs come to favor somatofugal motion? The small dendritic diameter of fine proximal dendrites $0.28\text{--}1.46\ \mu\text{m}$ [18] of SACs with a small volume-to-surface ratio would favor metabolic pump currents and exchanger currents in maintaining

ionic fluxes, thereby effecting $[Ca^{2+}]_i$ levels [6], yet co-transporters are too sluggish to detect moving stimuli in the operation of direction selectivity. Euler *et al.* [4] had shown $[Ca^{2+}]_i$ increases in the distal part of each dendrite that occurred independently of each other. There are two possible routes for the influx of Ca^{2+} ions into the distal varicosities of SACs: (i) through the plasmalemmal channels (i.e., plasma membrane containing Ca^{2+} -dependent ionic channels), and (ii) efflux from the endoplasmic reticulum (ER) where Ca^{2+} release is mediated by ryanodine receptors (RyRs) (i.e., intracellular Ca^{2+} channels) on the ER activated by increased $[Ca^{2+}]_i$ levels.

Studies on acutely isolated amacrine cells by enzymatic dissociation of the retina confirm local Ca^{2+} release to be located in dendrites primarily via nearby RyRs on the ER [21] which were also shown to promote synaptic transmission mediated by inositol 1,4,5-trisphosphate receptors (IP_3 Rs) by way of IP_3 -induced calcium release (IICR) mechanism [30]. Starburst amacrine cells have pre- and postsynaptic sites that are spatially intermingled and synaptic mitochondria can be found within $1\ \mu m$ of presynaptic active zones, mitochondrial Ca^{2+} transport (efflux of Ca^{2+} from mitochondria) interacts with Ca^{2+} transport mechanisms on the ER by stimulating the opening of adjacent RyRs receptors for release of Ca^{2+} ions from stores via Ca^{2+} -induced Ca^{2+} release (CICR) [14, 21]. This results in a rather slow-moving Ca^{2+} waves activated by CICR as a consequence of Ca^{2+} ions flooding the cytoplasm. Moreover, intracellular Ca^{2+} waves arise from the process of CICR from channels in the ER coupled to the diffusion of Ca^{2+} in the cytosol.

Waves in spatially extended cell models are of particular importance when studying the propagation of Ca^{2+} waves in SACs. In SACs, it is still yet to be proven experimentally if they possess a continuous ER in which the lumen would be free of both RyRs and IP_3 Rs receptors because these are found only on discrete ER, or whether the cytoplasm does not act as a continuing homogenous excitable medium to generate Ca^{2+} release, but instead releasing events occur at discrete sites a few micrometers apart, which serve as local sources of Ca^{2+} , termed “sparks” (i.e., clusters of RyRs receptors). Calcium signals in the form of waves are composed of elementary release events (Ca^{2+} sparks) from such spatially localized Ca^{2+} stores, where Ca^{2+} diffuses from the cell membrane to the nearby ER and binds to RyRs receptors which can open and release Ca^{2+} ions from the ER which in turn activates more RyRs receptors to open more Ca^{2+} channels, and cause a fast release of Ca^{2+} ions from local stores. This Ca^{2+} signal is ended when $[Ca^{2+}]_i$ levels become large and the Ca^{2+} pumps remove Ca^{2+} ions from the intracellular space into the ER and out of the cell. This constitutes a Ca^{2+} signal that is cyclic if the intracellular concentration of RyRs mediated Ca^{2+} release is larger than a threshold. Thus, RyRs mediated $[Ca^{2+}]_i$ levels below the threshold are not coded in a Ca^{2+} signal. However, to simplify the CICR mechanism, Ca^{2+} feedback can be used as CICR without the formation of RyRs mediated Ca^{2+} signals.

Is such a mechanism responsible for the Ca^{2+} bias to somatofugal motion in SACs? If somatic Ca^{2+} waves are driven by somatofugal motion, then all dendrites would have almost the same Ca^{2+} concentration over a distance of the SAC dendrite of approximately $100\text{ }\mu\text{m}$ [29]. This has been shown in hippocampal dendrites where metabotropic glutamate receptor activation induces Ca^{2+} waves [11]. Our aim is to show whether a CICR mechanism can sustain constant Ca^{2+} wave propagation in the somatofugal direction in order to act as the veto mechanism with a 100 ms-delay for the operation of retinal direction selectivity as illustrated in Fig. 1.

During the CICR mechanism, there are several processes that will affect $[\text{Ca}^{2+}]_i$ levels. Calcium uptake from the cytoplasm is through pumping and buffering mechanisms working against a recurrent leak of Ca^{2+} ions from the internal stores and from the extracellular fluid through voltage-gated Ca^{2+} channels, and release from internal stores such as ER, which can either be a discrete or a continuous membrane-delimited endogenous structure. Endogenous Ca^{2+} -binding proteins (e.g., calmodulin) produced in a variety of endogenous structures and other exogenous Ca^{2+} buffers effect (slow down) the propagation of Ca^{2+} waves. It is an open question whether buffering as a mechanism of Ca^{2+} uptake, which is ubiquitous in all living cells, is done in the SACs. There are no experimental findings to confirm the presence of buffering machinery in SACs from the intact retina [7]. This Ca^{2+} excitability is the physiological basis for propagating waves that can be experimentally tested via confocal microfluorimetry [5]. Pumps are found both on the plasma membrane and on the surface of the ER. Calcium ions are sequestered into

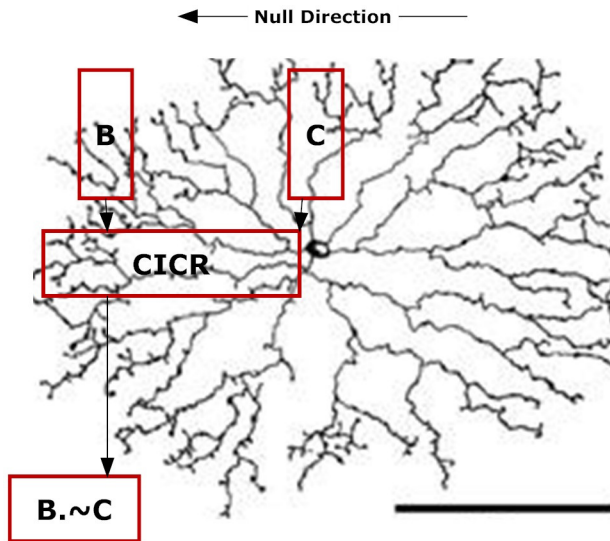


Fig. 1. Calcium-induced calcium release (CICR) scheme proposed. The bipolar B normally excites the underlying dendrites of the ganglion cell, while a wave of CICR has been initiated more centrally along a SAC's dendrite by excitation at C and arrives on time to veto the bipolar input through reciprocal synapses with the tips of the dendrites of the SAC. Scale bar = $100\text{ }\mu\text{m}$.

the ER by sacro-endoplasmic reticulum Ca^{2+} ATPase (SERCA) pumps under normal physiological conditions. Pumps which are embedded in the membrane consume nucleotide triphosphates and pump the Ca^{2+} ions up the gradient from the cytosol back into stores.

2. Modeling Ca^{2+} Release as a Threshold Process from the ER to the Cytosol

The effects of ionic flux due to the electric field in the cytosol (i.e., cytosolic voltage gradients) can be ignored and mainly account for the electrodiffusional forces due to movements of Ca^{2+} ions across the membrane at discrete points which leads to current flow (see [10, 13, 22, 23]). This assumption of ignoring ionic flux due to the electric field in the cytosol is done through regular electrodiffusion modeling, which assume that spatial variation of ionic concentration changes are small. When large ionic fluxes occur during retinal direction selectivity, the assumption does not imply small concentration changes occur as is often the case when the concentration gradient term is absent, but rather the membrane potential is so small such that cytosolic voltage gradients can be ignored. The partial differential equation describing the concentration of Ca^{2+} in the starburst dendrite must therefore be represented through a system of reaction-diffusion equations and not the cable equation or electrodiffusion equation. Electrodiffusion models in the absence of cytosolic voltage gradients apply to ionic diffusion across a membrane not within it since the movement of ions in response to a concentration gradient occurs across an interface like a cell membrane, while the cable equation is based on ionic concentrations being constant during electrical activity.

Calcium wave propagation due to the CICR process is described by a four-state kinetic model [3, 17, 25]. A fire-diffuse-fire model of wave propagation simplifies the kinetics by treating buffers phenomenologically [2, 12]. All buffers are assumed to be fast so that their presence can be modeled by an effective diffusion coefficient [2, 22]. Buffer-mediated Ca^{2+} diffusion in the cytosol plays a crucial role in the process. For CICR to occur, Ca^{2+} ions needs to diffuse between release sites. Release and intersite diffusion occur simultaneously with buffering that prevent $[\text{Ca}^{2+}]_i$ from building up. Realistic models of Ca^{2+} dynamics must account for their presence. Strier *et al.* [26] were the first to add buffers explicitly to the fire-diffuse-fire model. They then performed the standard reduction that leads to the rapid buffering approximation. Though important for their effect on the Ca^{2+} distribution, the spatiotemporal behavior of buffers themselves is not of importance. For this reason, different ways of simplifying the description of buffers is undertaken.

Fire-diffuse-fire models use a threshold process to mimic the nonlinear properties of Ca^{2+} channels [13, 31]. The Ca^{2+} release at a site releases Ca^{2+} ions instantaneously when the value of $[\text{Ca}^{2+}]_i$ at the site exceeds a threshold value. The release events (Ca^{2+} sparks) lead to the propagation of waves via diffusion of Ca^{2+} (diffuse). The model is highly nonlinear because the release events are implicitly determined

by the times when the $[\text{Ca}^{2+}]_i$ at a release site takes on the threshold value. The actions of pumps that resequence the Ca^{2+} ions back to the stores are neglected since pumps operate on a slower time scale. The limitation of the fire-diffuse-fire model is that the dynamics of the buffering is not included in the model formulation. A single equation governs the dynamics of buffered Ca^{2+} diffusion, rather than the more realistic coupled equations governing the dynamics of buffered and buffer-bound Ca^{2+} diffusion. Thul *et al.* [27, 28] presented a mathematical analysis of a bidomain threshold-release model of propagating Ca^{2+} waves observed when Ca^{2+} ions are released from internal stores (e.g., ER). Their bidomain model included equations for concentrations of intracellular and ER Ca^{2+} . However, in this paper, the dynamics of buffered Ca^{2+} diffusion is designated as a “*bidomain*” in the sense that two dependent variables are used in the formulation of the model, although physically we are dealing only with a single domain.

3. The Model Equations

We consider the release of Ca^{2+} from intracellular organelles, in particular the ER through Ca^{2+} feedback. The model includes simple Ca^{2+} dynamics resulting from intracellular buffering and Ca^{2+} extrusion. The present model serves as a starting point to further analyze Ca^{2+} excitability changes. To explore spatial aspects of Ca^{2+} signaling we include a single buffer species and the diffusive movement of Ca^{2+} ions, assuming Fick’s law applies in a homogeneous, isotropic one-dimensional cable structure for which the equation governing the dynamics of buffered Ca^{2+} diffusion is given by

$$\begin{aligned} \frac{\partial[\text{Ca}^{2+}]_i}{\partial t} = D_{\text{Ca}} \frac{\partial^2[\text{Ca}^{2+}]_i}{\partial x^2} - \text{Buffer} + J_{\text{leak}} \\ - P([\text{Ca}^{2+}]_i) + \nu_{\text{CICR}} H([\text{Ca}^{2+}]_i - C_T), \end{aligned} \quad (1)$$

where x is physical distance along the cable (cm), t is time (sec), D_{Ca} is the diffusion constant of free Ca^{2+} ($\mu\text{m}^2/\text{sec}$), “Buffer” is defined in §3.1, ν_{CICR} is the Ca^{2+} current density through channels ($\mu\text{M}/\text{sec}$), $J_{\text{leak}} = V_{\text{leak}} ([\text{Ca}^{2+}]_o - [\text{Ca}^{2+}]_i) > 0$ is the leak Ca^{2+} influx with $[\text{Ca}^{2+}]_o$ representing the external Ca^{2+} concentration at rest (mM), V_{leak} is the leak flux constant (sec^{-1}), C_T is the channel activation threshold (μM), and H is the Heaviside-step function. See Table 1 for all the constants defining the model. Note that Eq. (1) is nonlinear because the release events are implicitly determined by the times at which Ca^{2+} density at a release site takes on the threshold value C_T .

For the Ca^{2+} homeostasis to be maintained, the Ca^{2+} -buffering does not reduce all the intracellular Ca^{2+} , and the remaining Ca^{2+} ions must be removed by two transport systems: (i) a Na^+ -dependent Ca^{2+} efflux (i.e., Na^+ - Ca^{2+} exchanger system), in which the energy required for the extrusion of Ca^{2+} ions is derived from the inward movement of Na^+ ions down their concentration gradient; (ii) Ca^{2+} -extrusion system (ATP-driven pump) that requires ATP, an energy source activated at low

Table 1. List of symbols

$[Ca^{2+}]_i$	intracellular calcium concentration (μM), where $M \equiv \text{mol m}^{-3}$
$[Ca^{2+}]_o$	external calcium concentration at rest (μM)
x	physical distance along dendrite (cm)
t	time (sec)
D_{Ca}	diffusion constant of free calcium ($\mu m^2/\text{sec}$)
V_{leak}	leak flux constant (sec^{-1})
C_T	channel activation threshold (μM)
C_0	initial calcium concentration (μM)
ν_{CICR}	calcium current density through channels ($\mu M/\text{sec}$)
P_m	pump rate (m/sec)
K_p	pump dissociation constant (μM)
d	diameter of dendrite (cm)
$[B]_{total} (= [CaB] + [M])$	total concentration of calcium binding (μM)
$[CaB]$	concentration of bound buffer (μM)
$[M]$	concentration of unbound buffer (μM)
f	forward reaction rate ($\mu M^{-1} \text{msec}^{-1}$)
b	backward reaction rate (msec^{-1})
$K_D = b/f$	dissociation constant (μM)
D_m	diffusion constant of buffered calcium ($\mu m^2/\text{sec}$)
$k = K_D[B]_{total}/([Ca^{2+}]_i)^2$	buffer capacity (dimensionless)
$k_0 = [B]_{total}/K_D$	buffer capacity under the EBA (dimensionless)
$\gamma = 4P_m/d$	constant parameter (sec^{-1})
ℓ	physical length along dendrite (cm)
G	Green's function ($\mu M/\text{cm}$)
\hat{G}	Green's function (μM)
w	heat functional (μM)
t_i	time when the concentration equals the threshold (sec)
α	thermal diffusivity constant (cm^2/sec)
ε	perturbation parameter (dimensionless)
$H[\cdot]$	Heaviside step-function (dimensionless)
$\delta[\cdot]$	Dirac-delta function (inverse dimension of its argument)

values of $[Ca^{2+}]_i$. The extrusion or re-uptake into the stores of Ca^{2+} ions is through pumps which are assumed to be homogeneously distributed over the plasma membrane, active at low values of $[Ca^{2+}]_i$. The Ca^{2+} pump (ATP-operated) is a high-affinity, low-capacity pump that can cause an output current and is governed by Hill-type equation:

$$P([Ca^{2+}]_i) = \frac{4P_m}{d} K_p \frac{[Ca^{2+}]_i}{[Ca^{2+}]_i + K_p}, \quad (2)$$

where P_m is the membrane pump parameter (m/sec), K_p (μM) is the pump dissociation constant and the factor $4/d$ is the surface area-to-volume ratio for a cable of diameter d (cm). In the absence of leakage, the resting value of $[Ca^{2+}]_i$ is taken to zero. Note that a constant leakage rate can always be absorbed by defining the concentration relative to the resting level.

3.1. The excess buffer approximation

Neher [15] was first to assume that for a single mobile buffer, it does not have to change its concentrations by binding to Ca^{2+} , a reasonable approximation if a high concentration of mobile buffer is present. This has come to be known as the excess buffer approximation (EBA). The assumption of unsaturability of Ca^{2+} buffer is likely to be valid when Ca^{2+} buffer is in excess or Ca^{2+} concentration is low. Since many types of amacrine cells, including SACs, release transmitter tonically without the need for spikes, requiring only a modest increase in $[\text{Ca}^{2+}]_i$ from the ER, it would seem that EBA is a valid approximation [16]. Our analytical approach is based on linearized approximations valid for Ca^{2+} transients of small amplitude as observed in SACs [4].

Our simple model of Ca^{2+} dynamics assumes that Ca^{2+} binds to a single binding site on the endogenous buffer. The rate of change of $[\text{Ca}^{2+}]_i$ is dependent on the reversible binding with soluble buffering proteins. The buffering proteins are considered immobile (non-diffusible) and uniform throughout the dendrite. Mobility of the buffer is important because stationary buffers at high concentrations will eventually be saturated near a source. The key assumption is that sufficient mobile buffer can diffuse to the source to replenish the free buffer that becomes bound. The total concentration of Ca^{2+} binding sites is denoted as $[\text{B}]_{\text{total}}$ and it is the sum of the concentrations of free (unbound) $[\text{M}]$ and bound $[\text{CaB}]$ forms of the buffer present, all measured in μM . If we assume that $[\text{B}]_{\text{total}}$ is uniformly distributed over space, we can work only with two variables $[\text{Ca}^{2+}]_i(x, t)$ and $[\text{CaB}](x, t)$, since under EBA $[\text{B}]_{\text{total}}$ is high enough such that it may be assumed to be a constant. The spatiotemporal evolution of the cytosolic Ca^{2+} concentration is described by only two equations governing $[\text{Ca}^{2+}]_i$ and $[\text{CaB}]$, which are to be solved subject to boundary and initial condition. The rate at which Ca^{2+} binds to proteins is proportional to $[\text{Ca}^{2+}]_i$ and the concentration of free binding sites. Calcium also dissociates from the buffer protein at a rate proportional to the concentration of the complex. Thus the rate at which Ca^{2+} binds to protein buffering is represented by:

$$\frac{\partial[\text{CaB}]}{\partial t} = D_M \frac{\partial^2[\text{CaB}]}{\partial x^2} + f([\text{B}]_{\text{total}} - [\text{CaB}])[\text{Ca}^{2+}]_i - b[\text{CaB}],$$

where $f(\mu\text{M}^{-1} \text{msec}^{-1})$ and $b(\text{msec}^{-1})$ are the forward and backward reaction rates, respectively, of the binding reaction, D_M is the diffusion constant of buffered Ca^{2+} ($\mu\text{m}^2/\text{sec}$), and $[\text{B}]_{\text{total}} = [\text{CaB}] + [\text{M}]$ is the total concentration of Ca^{2+} binding (μM) with $[\text{CaB}]$, and $[\text{M}]$ being the concentration of bound and unbound forms of the buffer present, respectively. As a consequence, our attention is in knowing the value of $[\text{Ca}^{2+}]_i$ bound to the buffer $[\text{CaB}]$ when the buffer capacity is $k([\text{Ca}^{2+}]_i) = K_D[\text{B}]_{\text{total}}/(K_D + [\text{Ca}^{2+}]_i)^2$, where K_D is the dissociation constant ($= b/f$) in μM ,

so that the diffusion of buffer-bound Ca^{2+} $[\text{CaB}]$ satisfies

$$\begin{aligned} \frac{\partial[\text{CaB}]}{\partial t} = D_M \frac{\partial^2[\text{CaB}]}{\partial x^2} - (f[\text{B}]_{\text{total}}/k) \frac{[\text{CaB}]}{(1 + [\text{Ca}^{2+}]_i/K_D)} \\ + f[\text{B}]_{\text{total}}[\text{Ca}^{2+}]_i. \end{aligned} \quad (3)$$

When the buffer is not saturated, i.e., $[\text{Ca}^{2+}]_i \ll K_D$, the buffer capacity $k([\text{Ca}^{2+}]_i)$ then reduces to $k_0 = [\text{B}]_{\text{total}}/K_D$ so that the diffusion of buffer-bound Ca^{2+} expressed by Eq. (3) simplifies to the following:

$$\frac{\partial[\text{CaB}]}{\partial t} = D_M \frac{\partial^2[\text{CaB}]}{\partial x^2} - (f[\text{B}]_{\text{total}}/k_0)[\text{CaB}] + f[\text{B}]_{\text{total}}[\text{Ca}^{2+}]_i. \quad (4)$$

The right-hand side of Eq. (4) (without the spatial diffusion term) replaces the “*Buffer*” term in Eq. (1) which leads to a linearized equation for $[\text{Ca}^{2+}]_i$:

$$\begin{aligned} \frac{\partial[\text{Ca}^{2+}]_i}{\partial t} = D_{\text{Ca}} \frac{\partial^2[\text{Ca}^{2+}]_i}{\partial x^2} + (f[\text{B}]_{\text{total}}/k_0)[\text{CaB}] - f[\text{B}]_{\text{total}}[\text{Ca}^{2+}]_i \\ - \gamma[\text{Ca}^{2+}]_i + \nu_{\text{CICR}} H [([\text{Ca}^{2+}]_i - C_T)], \end{aligned} \quad (5)$$

where $\gamma = 4P_m/d$ is a constant under the assumption that the value of $[\text{Ca}^{2+}]_i$ is much lower than the dissociation constant K_D (i.e., $[\text{Ca}^{2+}]_i \ll K_D$) and the pump extrudes endogenous Ca^{2+} in a linear fashion, viz.

$$\lim_{[\text{Ca}^{2+}]_i \ll K_D} P([\text{Ca}^{2+}]_i) \rightarrow \gamma[\text{Ca}^{2+}]_i.$$

By including the effect of pumps, we can study how the wave-front propagates (via $\partial[\text{Ca}^{2+}]_i/\partial x$), as well as how $[\text{Ca}^{2+}]_i$ goes back to its basal level. Note that in the absence of leakage, the basal level is zero, but the basal level can be defined by absorbing the γ with V_{leak} and letting $[\text{Ca}^{2+}]_o = 0$ (i.e., Ca^{2+} isopotentiality in the extracellular medium).

3.2. Analytical solution of the reaction-diffusion system

The resulting Ca^{2+} system under the EBA in the vicinity of the buffer where we assume $[\text{B}]_{\text{total}}$ to be constant is described by a system of two coupled non-homogeneous quasilinear reaction-diffusion equations:

$$\begin{aligned} \frac{\partial[\text{Ca}^{2+}]_i}{\partial t} = D_{\text{Ca}} \frac{\partial^2[\text{Ca}^{2+}]_i}{\partial x^2} - (\gamma + f[\text{B}]_{\text{total}})[\text{Ca}^{2+}]_i + \left(\frac{f[\text{B}]_{\text{total}}}{k_0} \right) [\text{CaB}] \\ + \nu_{\text{CICR}} H [([\text{Ca}^{2+}]_i - C_T)] \end{aligned} \quad (6)$$

$$\frac{\partial[\text{CaB}]}{\partial t} = D_M \frac{\partial^2[\text{CaB}]}{\partial x^2} - (f[\text{B}]_{\text{total}}/k_0)[\text{CaB}] + f[\text{B}]_{\text{total}}[\text{Ca}^{2+}]_i. \quad (7)$$

The solution of the coupled quasilinear reaction-diffusion Eqs. (6) and (7) can be obtained from solutions of the “classical” diffusion equation and satisfy the same

boundary conditions as the original problem [8]. Letting $u(x, t) = \partial[\text{Ca}^{2+}]_i / \partial x$ and differentiating Eq. (6) with respect to x we obtain:

$$u_t = D_{\text{Ca}} u_{xx} - (\gamma + f[\text{B}]_{\text{total}})u + \frac{f[\text{B}]_{\text{total}}}{k_0} \frac{\partial[\text{CaB}]}{\partial x} + \nu_{\text{CICR}} \delta ([\text{Ca}^{2+}]_i - C_{\text{T}})u. \quad (8)$$

where subscripts x and t denote partial derivatives with respect to these variables.

Now $[\text{Ca}^{2+}]_i(x, t) = \int u(\xi, t) d\xi$ where $u(x, t)$ satisfies a nonlinear Volterra integral equation:

$$u(x, t) = \nu_{\text{CICR}} \int_0^\ell \int_0^t G(x, \xi; t-s) \delta ([\text{Ca}^{2+}]_i(\xi, s) - C_{\text{T}}) u(\xi, s) d\xi ds, \quad (9)$$

where ℓ is the physical length along the cable (cm) and $G \equiv \lim_{\nu_{\text{CICR}} \rightarrow 0} \{\partial[\text{Ca}^{2+}]_i / \partial x\}$ is the Green's function, viz.

$$\partial G / \partial t = D_{\text{Ca}} \partial^2 G / \partial x^2 - (\gamma + f[\text{B}]_{\text{total}})G + (f[\text{B}]_{\text{total}} / k_0) \partial[\text{CaB}] / \partial x. \quad (10)$$

The coupled system Eqs. (7) and (10) can be solved analytically using classical methods employed by Hill [9] to yield an expression for Green's function:

$$\begin{aligned} G(x, \xi; t) &= e^{-(\gamma + f[\text{B}]_{\text{total}})t} w_x(x, t) + \sqrt{\frac{f[\text{B}]_{\text{total}}}{k_0}} \left(\frac{e^{\lambda t}}{D_{\text{Ca}} - D_{\text{m}}} \right) \int_{D_{\text{m}} t}^{D_{\text{Ca}} t} e^{-\mu p} \\ &\times \left\{ \sqrt{f[\text{B}]_{\text{total}}} \left(\frac{D_{\text{m}} t - p}{p - D_{\text{Ca}} t} \right)^{1/2} I_1(\eta) w_x(x, t) + \sqrt{\frac{f[\text{B}]_{\text{total}}}{k_0}} I_0(\eta) w_x^*(x, p) \right\} dp, \end{aligned} \quad (11)$$

where I_0, I_1 are modified Bessel function of order zero and one, respectively, and the constants (λ, μ, η) are defined as follows:

$$\begin{aligned} \lambda &= \frac{(\gamma + f[\text{B}]_{\text{total}})D_{\text{m}} - \frac{f[\text{B}]_{\text{total}}}{k_0} D_{\text{Ca}}}{D_{\text{Ca}} - D_{\text{m}}} \\ \mu &= \frac{f[\text{B}]_{\text{total}}(1 - 1/k_0) + \gamma}{D_{\text{Ca}} - D_{\text{m}}} \\ \eta &= \frac{2f[\text{B}]_{\text{total}}}{\sqrt{k_0}(D_{\text{Ca}} - D_{\text{m}})} \{(D_{\text{Ca}} t - p)(p - D_{\text{m}} t)\}^{1/2}, \end{aligned} \quad (12)$$

with p being a constant of integration. The heat functions $w(x, t)$ and $w^*(x, t)$ are solutions of the heat equation where w^* is the solution of the heat equation $w(x, t)$ via $w^* = e^{\gamma + f[B]_{\text{total}}} w(x, t)$, with $w(x, t)$ satisfying the heat equation:

$$\partial w / \partial t = \alpha^2 \nabla^2 w,$$

where α is a constant known as the thermal diffusivity (cm^2/sec). The solution for the case of sealed-ends, subject to initial condition $w(0, 0) = [\text{Ca}^{2+}]_{\text{rest}}$ where $[\text{Ca}^{2+}]_{\text{rest}} = c_o$ readily follows

$$w(x, t) = c_o \left\{ 1 + 2 \sum_{n=1}^{\infty} \cos(n\pi x/\ell) \exp(-[n\pi\alpha/\ell]^2 t) \right\}. \quad (13)$$

Recasting Eq. (9) into a nonlinear integral Volterra equation:

$$u(x, t) = \nu_{\text{CICR}} \int_0^t G(x, \xi; t-s) f[u(\xi, s)] ds, \quad (14)$$

where

$$f[u(\xi, s)] = \int_0^\ell \delta([\text{Ca}^{2+}]_i(\xi, s) - C_T) u(\xi, s) d\xi.$$

A solution of Eq. (14) can be found via a regular perturbation series expansion about $G(x, \xi, t)$ where upon substituting

$$u(x, t) = \sum_{n=0}^{\infty} \varepsilon^n u_n(x, t)$$

into Eq. (14), expanding $f(\cdot)$ via Taylor expansion, and equating coefficients in powers of ε , leading to a two-term asymptotic expansion:

$$u(x, t) = u_o(x, t) + \varepsilon u_1(x, t) + o(\varepsilon^2),$$

where

$$u_o(x, t) = G(x, \xi; t)$$

$$u_1(x, t) = \nu_{\text{CICR}} \int_0^t G(x, \xi; t-s) f[u_o(\xi, s)] ds.$$

Now substituting the above we find the solution to Eq. (14) becomes

$$\begin{aligned} u(x, t) = & G(x, \xi; t) + \varepsilon \nu_{\text{CICR}} \int_0^\ell \int_0^t G(x, \xi; t-s) \\ & \times \delta([\text{Ca}^{2+}]_i(\xi, s) - C_T) u_o(\xi, s) d\xi ds + O(\varepsilon^2). \end{aligned}$$

Using the semigroup property of the Green's function, it can be shown that a two-term asymptotic expansion for the regime in which the buffer does not saturate is

$$u(x, t) = G(x, \xi; t) + \varepsilon \nu_{\text{CICR}} \int_0^t \delta([\text{Ca}^{2+}]_i(\xi, s) - C_T) ds G(x, y; t) + O(\varepsilon^2), \quad (15)$$

where source occurs at $x = \xi$ and $x = y$ where points ξ and y are adjacent to each other. If $[\text{Ca}^{2+}]_i(x, t) > C_T$ at point $x = \xi$ then Ca^{2+} source occurs at $x = y$ where points y and ξ are juxtaposed. Consequently, in the case of EBA, buffered diffusion of Ca^{2+} is given by:

$$[\text{Ca}^{2+}]_i(x, t) = \hat{G}(x, \xi; t) + \epsilon\nu_{\text{CICR}} \int_0^t \delta([\text{Ca}^{2+}]_i(\xi, s) - C_T) ds \hat{G}(x, y; t), \quad (16)$$

where \hat{G} is identical to G with $w_x(x, t)$ replaced by $w(x, t)$, and t_i are the times when the Ca^{2+} concentration equals the threshold.

If we expand the Dirac-delta function as a function of $[\text{Ca}^{2+}]_i$ and replace $[\text{Ca}^{2+}]_i$ with \hat{G} to allow for continuity of Ca^{2+} transients at $t = t_1$, then by evaluating the derivative of the Ca^{2+} transient at $t = t_2$, brings us to the final result for the buffered diffusion of Ca^{2+} :

$$[\text{Ca}^{2+}]_i(x, t) = \hat{G}(x, \xi; t) + \epsilon\nu_{\text{CICR}} \left\{ \frac{H(t - t_1)}{\left| \frac{d\hat{G}}{dt_1}(x, \xi; t_1) \right|} + \frac{H(t - t_2)}{\left| \frac{d[\text{Ca}^{2+}]_i}{dt_2}(\xi, t_2) \right|} \right\} \hat{G}(x, y; t), \quad (17)$$

where

$$\begin{aligned} \frac{d[\text{Ca}^{2+}]_i}{dt_2}(x, t_2) &= \frac{d\hat{G}}{dt_2}(x, \xi; t_2) + \epsilon\nu_{\text{CICR}} \\ &\times \left\{ \frac{\delta(t_2 - t_1)\hat{G}(x, \xi; t_2)}{\left| \frac{d\hat{G}}{dt_1}(x, \xi; t_1) \right|} + \frac{H(t_2 - t_1)}{\left| \frac{d\hat{G}}{dt_1}(x, \xi; t_1) \right|} \frac{d\hat{G}}{dt_2}(x, \xi; t_2) \right\}. \end{aligned}$$

With t_1 and t_2 are found when $\hat{G}(x, \xi; t_1) = C_T$ and

$$\hat{G}(x, \xi; t_2) + \epsilon\nu_{\text{CICR}} \frac{H(t_2 - t_1)}{\left| \frac{d\hat{G}}{dt_1}(x, \xi; t_1) \right|} \hat{G}(x, y; t_2) = C_T$$

respectively. To measure the wave-speed of Ca^{2+} in the presence of buffer, the normalized $[\text{Ca}^{2+}]_i$ governed by Eq. (17) is recorded at four equidistant points along a dendrite. The speed is defined to be the distance between any two locations; the wave is measured divided by the spacing between the curves of the normalized $[\text{Ca}^{2+}]_i$ measured at half-amplitude.

Wyatt and Daw [32] (see also [29] in the avian retina) found receptive field of a directionally selective ganglion cells to be cardioid in shape with the inhibitory region displaced toward the side where the null sweep starts relative to the excitatory regions. Biophysical mechanisms for delayed suppression of direction selectivity maximally at around 100 ms delay [29] are yet unknown. Barlow [1] hypothesized that CICR mechanism is the biophysical mechanism underlying this delay. Hence, we can test this hypothesis using Eq. (17) to see whether a Ca^{2+} wavefront can propagate from the soma at $x = 0$ to the distal end of the dendrite at $x = \ell$ in under 100 msec.

The system of reaction-diffusion equations under the EBA is not translationally invariant, so wave-like propagating solutions can vary between continuous and saltatory propagation. Calcium sources if significantly increased will lead to propagation failure in the somatopetal direction due to the build-up of Ca^{2+} excitability [20]. This may provide quantitative support for CICR mechanism in SACs based on a transition between propagation success and its failure depending on the heterogeneity of the Ca^{2+} source.

The simulation of the CICR-based Ca^{2+} waves in the presence of unsaturated buffer will be presented elsewhere.

4. Simulation of Luminal Ca^{2+} Diffusion in the Absence of Buffer

The luminal Ca^{2+} diffusion speed in the absence of buffer predicated by the fire-diffuse-fire model [24]:

$$v_{\text{Ca}} = 4(D/\xi) \log[\sigma/(\xi C_T)], \quad (18)$$

where D is the diffusion coefficient of Ca^{2+} ($\mu\text{m}^2/\text{sec}$); σ is the number of Ca^{2+} ions released; C_T is the threshold value of $[\text{Ca}^{2+}]_i$ (μM), and ξ is the site spacing (μm). Equation (18) is valid for $C_T\xi/\sigma \ll 1$ in the absence of buffers or for rapid buffer approximation. If the sites are too far apart or too weak or the threshold too high, there can be no propagating waves. In the absence of buffers, binding to buffers is assumed instantaneous and the effect of buffering is reflected in the values of D being different to the diffusion coefficient D_{Ca} in the presence of buffers. Typical values are $C_T = 0.2 \mu\text{M}$, $\sigma = 1.5 \times 10^{-7} \mu\text{mol}$, $D = 0.3 \mu\text{m}^2/\text{sec}$ and $\xi = 0.005 \mu\text{m}$.

In the absence of buffer, the luminal Ca^{2+} diffusion (giving the upper most range for speeds affected by buffering) enables a wave to travel $120 \mu\text{m}$ from the soma to the distal varicosities of SACs in 100 msec if the spacing between local sites of Ca^{2+} release is $0.005 \mu\text{m}$ apart, suggesting that a continuous ER is required throughout

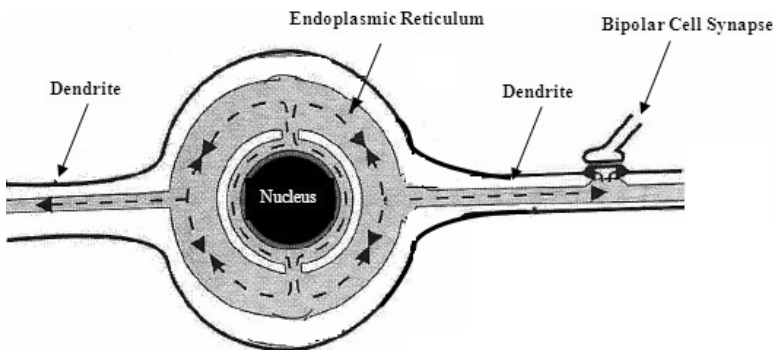


Fig. 2. A hypothetical model of the ER Ca^{2+} signaling in the somatofugal direction involving exogenous Ca^{2+} ions rapidly diffusing through the ER lumen, connecting the soma with the distal varicosities of SACs.

the span of the dendritic arbor (see Fig. 2). Supposedly this is significantly faster than CICR-based Ca^{2+} waves in the presence of unsaturated buffer.

Apart from the slowing of the propagating wavefront of Ca^{2+} in the presence of endogenous buffers, it is also possible that if local ER were to be present in the distal varicosities of SACs, then the intermediate dendritic zone would serve as a diffusion barrier for Ca^{2+} stores disconnected from the soma, prohibiting the ER to function as a tunnel for rapid Ca^{2+} transport. However, since the thickness of the smallest intermediate zone is $0.28\text{ }\mu\text{m}$ [18], and the bulk of ER in dendrites measures in the $0.02\text{ }\mu\text{m}$ range, which is smaller than the largest ER having a diameter of approximately $0.18\text{ }\mu\text{m}$, it would indicate that ER lumen connecting soma with the distal varicosities partially encapsulates the cytoplasm, so that $[\text{Ca}^{2+}]_{\text{ER}}$ incompletely replaces $[\text{Ca}^{2+}]_{\text{i}}$. A luminally connected ER model would be required for rapid luminal Ca^{2+} diffusion in the somatofugal direction. While Ca^{2+} signaling in the somatopetal direction involves exogenous Ca^{2+} ions reduced by the cellular inhibitory mechanisms (see [20]) possibly in the presence of Ca^{2+} -binding proteins released from the ER. Experimental studies will need to verify the existence of such a continuous lumen of the ER from the soma to the distal dendrites of SACs.

5. Conclusion

This study has facilitated in determining whether Ca^{2+} mobilization accounts for directional selectivity. It was theorized that Ca^{2+} signaling involves exogenous Ca^{2+} ions augmented by Ca^{2+} -binding proteins released from a continuously distributed ER in order for the veto time-delay to be within the expected values seen experimentally. Further work is needed to show whether the CICR-based propagating Ca^{2+} wavefront in the somatofugal direction is impeded by endogenous buffers. This would seriously put in doubt the machinery associated with CICR as a basis for directional selectivity [1] as it would seem from the analysis that rapid luminal Ca^{2+} diffusion gives propagation speeds which are more likely to be reflective of the functioning of SACs in retinal direction selectivity and that Ca^{2+} source heterogeneity is the cause of directionally selective Ca^{2+} responses in SACs.

Acknowledgments

The research was founded by a University of Malaya grant (RCG 033-09ICT).

References

- [1] Barlow H, Intraneuronal information processing, directional selectivity and memory for spatio-temporal sequences, *Network: Comput Neural Syst* **7**:251–259, 1996.
- [2] Dawson SP, Keizer J, Pearson JE, Fire-diffuse-fire model of dynamics of intracellular calcium waves, *Proc Natl Acad Sci USA* **96**:6060–6063, 1999.
- [3] Dupont G, Berridge MJ, Goldbeter A, Signal induced Ca^{2+} oscillations: Properties of a model based on Ca^{2+} -induced Ca^{2+} release, *Cell Calcium* **12**:73–86, 1991.

- [4] Euler T, Detwiler PB, Denk W, Directionally selective calcium signals in dendrites of starburst amacrine cells, *Nature* **418**:845–852, 2002.
- [5] Euler T, Hausselt SE, Margolis DJ, Breuninger T, Castell X, Detwiler PB, Denk W, Eyecup scope-optical recordings of light stimulus-evoked fluorescence signals in the retina, *Pflugers Arch* **457**:1393–1414, 2009.
- [6] Gavrikov KE, Dmitriew AV, Keyser KT, Mangel SC, Cation-chloride cotransporters mediate neural computation in the retina, *Proc Natl Acad Sci USA* **100**:16047–16052, 2003.
- [7] Hausselt SE, Euler T, Detwiler PB, Denk W, A dendrite-autonomous mechanism for direction selectivity in retinal starburst amacrine cells, *PLoS Biol* **5**:e185, 2007.
- [8] Hill JM, Aifantis EC, On the theory of diffusion in media with double diffusivity II. Boundary-value problems, *Q J Mech Appl Math* **33**:23–41, 1980.
- [9] Hill JM, On the solution of reaction-diffusion equations, *IMA J Appl Math* **27**:177–194, 1981.
- [10] Iannella N, Tanaka S, Analytical solutions for nonlinear cable equations with calcium dynamics, I: Derivations, *J Integr Neurosci* **5**:249–272, 2006.
- [11] Jaffe DB, Brown TH, Metabotropic glutamate receptor activation induces calcium waves within hippocampal dendrites, *J Neurophysiol* **72**:471–474, 1994.
- [12] Keizer J, Smith G, Dawson SP, Pearson J, Saltatory propagation of Ca^{2+} waves by Ca^{2+} sparks, *Biophys J* **75**:595–600, 1998.
- [13] Kupferman R, Mitra PP, Hohenberg PC, Wang SS, Analytical calculation of intracellular calcium wave characteristics, *Biophys J* **72**:2430–2444, 1997.
- [14] Mitra P, Slaughter MM, Mechanism of generation of spontaneous miniature outward currents (SMOCs) in retinal amacrine cells, *J Gen Physiol* **119**:355–372, 2002.
- [15] Neher E, Concentration profiles of intracellular calcium in the presence of a diffusible chelator, in Heinemann U, Klee M, Neher E, Singer W (eds.), *Calcium Electrogenesis and Neuronal Functioning*, Springer, Berlin, 1986.
- [16] Neher E, Usefulness and limitations of linear approximations to the understanding of Ca^{2+} signals, *Cell Calcium* **24**:345–357, 1998.
- [17] Pencea CS, Hentschel HGE, Excitable calcium wave propagation in the presence of localized stores, *Phys Rev E* **62**:8420–8426, 2000.
- [18] Poznanski RR, Modelling the electrotonic structure of starburst amacrine cells in the rabbit retina: A functional interpretation of dendritic morphology, *Bull Math Biol* **54**:905–928, 1992.
- [19] Poznanski RR, Biophysical mechanisms and essential topography of directionally selective subunits in rabbit's retina, *J Integr Neurosci* **4**:341–361, 2005.
- [20] Poznanski RR, Cellular inhibitory behavior underlying the formation of retinal direction selectivity in the starburst network, *J Integr Neurosci* **9**:299–335, 2010.
- [21] Sen M, McMains E, Gleason E, Local influence of mitochondrial calcium transport in retinal amacrine cells, *Vis Neurosci* **24**:1–16, 2007.
- [22] Shuai JW, Jung P, Sub-threshold Ca^{2+} waves, *New J Phys* **5**:132.1–132.20, 2003.
- [23] Shuai JW, Huang YO, Rudiger S, Pull-wave transition on an inhomogenous model for calcium signals, *Phys Rev E* **81**:041904, 2010.
- [24] Smith G, Pearson J, Keizer J, Modeling intracellular calcium waves and sparks, in Fall C, Marland E, Wagner J, Tyson J (eds.), *Computational Cell Biology*, Springer, New York, 2002.

- [25] Sneyd J, Girard S, Clapham D, Calcium wave propagation by Ca^{2+} -induced Ca^{2+} release: An unusual excitable system, *Bull Math Biol* **55**:315–344, 1993.
- [26] Strier DE, Ventura AC, Dawson SP, Saltatory and continuous calcium waves and the rapid buffering approximation, *Biophys J* **85**:3575–3586, 2003.
- [27] Thul R, Smith GD, Coombes S, A bidomain threshold model of propagating calcium waves, *J Math Biol* **56**:435–463, 2008.
- [28] Thul R, Coombes S, Smith GD, Sensitisation waves in a bidomain fire-diffuse-fire model of intracellular Ca^{2+} dynamics, *Physica D* **238**:2142–2152, 2009.
- [29] Uchiyama H, Kanaya T, Sonohata S, Computation of motion direction by quail retinal ganglion cells that have a nonconcentric receptive field, *Vis Neurosci* **17**:263–271, 2000.
- [30] Warrier A, Borges S, Dalcino D, Walters C, Wilson M, Calcium from internal stores triggers release from retinal amacrine cells, *J Neurophysiol* **94**:4196–4208, 2005.
- [31] Wang SS-H, Thompson SH, Local positive feedback by calcium in the propagation of intracellular calcium waves, *Biophys J* **69**:1683–1697, 1995.
- [32] Wyatt H, Daw N, Directionally sensitive ganglion cells in the rabbit retina: Specificity for stimulus direction, size, and speed, *J Neurophysiol* **38**:613–626, 1975.